Physica C 470 (2010) 782–785

Contents lists available at ScienceDirect

Physica C

journal homepage: www.elsevier.com/locate/physc

Deforming and moving a vortex by the tip of a magnetic force microscope

E.H. Brandt [a,*], G.P. Mikitik [a,b], E. Zeldov [c]

[a] Max Planck Institute for Metals Research, D-70506 Stuttgart, Germany
[b] B. Verkin Institute for Low Temperature Physics & Engineering, Kharkov 61103, Ukraine
[c] Dept. of Condensed Matter Physics, Weizmann Institute of Science, Rehovot 76100, Israel

ARTICLE INFO

Article history:
Available online 20 February 2010

Keywords:
Type-II superconductor
Pinning
Curved vortex
Magnetic force microscopy

ABSTRACT

Recent experiments [O.M. Auslaender et al., Nat. Phys. 5 (2009) 35] use a magnetic force microscope not only to image but also to move and deform an individual vortex line in a bulk YBCO type-II superconductor. The theory of this experiment is presented accounting for pinning and curving of the vortex and for the full three-dimensional anisotropy of pinning and of vortex line tension in this material.

© 2010 Elsevier B.V. All rights reserved.

Magnetic force microscopy (MFM) recently was employed [1] to image and manipulate individual vortices in a single crystal $YBa_2Cu_3O_{6.991}$, directly measuring the interaction of a moving vortex with the local pinning potential. When the magnetic tip of the MFM, kept at a height Z above the surface $z = 0$, was oscillated along x and moved slowly along y, an individual vortex was dragged such that its end at $(x_0, y_0, z = 0)$ performed a zigzag path that filled an approximately elliptical area stretched along y. Thus, the excursion of the vortex end perpendicular to the oscillation was much larger than the amplitude of the vortex oscillations. This strongly anisotropic response can be understood as described below; for details see [2]. Basically, the large excursion occurs since the transverse wiggling helps to depin the vortices.

We consider a single vortex of shape $x(z), y(z)$ inside a superconducting half space $z \leqslant 0$. The magnetic tip at position (X, Y, Z) may be modelled as a magnetic monopole of strength $\tilde{m}$ that exerts an attractive force $\mathbf{F}$ on the vortex end which may be approximated as a monopole of strength $2\Phi_0/\mu_0$ located at a depth λ [3]. If the tip is approximated as a long narrow ferromagnetic cylinder the magnetic monopole $\tilde{m}$ is the magnetic moment per unit length or the magnetization times cross section of this cylinder. As shown experimentally in Ref. [1], the attractive force is indeed described well by the expression obtained from this monopole model,

$$\mathbf{F} = q\frac{\mathbf{R} + (Z + h_0)\hat{\mathbf{z}}}{(R^2 + (Z + h_0)^2)^{3/2}} = (F_x, F_y, F_z), \tag{1}$$

where $\mathbf{R} \equiv (X - x_0, Y - y_0)$, the length $h_0 \approx \lambda$, and $q = \tilde{m}\Phi_0/2\pi$. It follows from Eq. (1) that when the distance R between the tip and the vortex increases, the lateral force (F_x, F_y) applied to the vortex increases, too. At $R_m = (Z + h_0)/\sqrt{2}$ this force reaches its maximum $F_m = 0.385q/(Z + h_0)^2$, and at a further increase of R the lateral force decreases and tends to zero at large R. The experiments [1] monitored the vortex position (x_0, y_0) by measuring $\partial F_z/\partial z$, which is maximum when the tip is just above the vortex end. For previous MFM manipulation of vortices see [4].

The horizontal dragging force density on the vortex is modelled as $\mathbf{f}_{ex}^{\parallel}(x, y, z) = (F_x, F_y)\exp(z/\lambda)/\lambda$, which is exact in the limit $R \gg \lambda$. The length λ is of the order of the in-plane London penetration depth $\lambda_{ab} = \sqrt{\lambda_a\lambda_b}$. For YBCO we take into account an anisotropy in the crystalline ab-plane $\zeta = \lambda_a/\lambda_b = 1.3$ and an $\epsilon = \lambda_{ab}/\lambda_c \ll 1$. The line tension of the vortex is assumed to be local, like the tension of a string. A refined theory should account for both an improved external force density and the nonlocal vortex line tension, see Eq. (4.13) of [5].

Initially, at times $t \leqslant 0$ the vortex is straight and pinned at $x = y = 0$. The attractive monopole–monopole force of the tip acting near the vortex end depins and curves the upper section $z > z_0$ of the vortex such that at each moment the vortex is in equilibrium. The vortex shape $x(z)$, $y(z)$ at time t is computed iteratively by moving each vortex segment such that the total force on it is zero, i.e., the sum of the densities of the external dragging force, of the elastic restoring force from the vortex line tension, and of the pinning force, is zero for all z. The depth of the vortex deformation, z_0, is also found in this calculation. At small tilt angles and in the limit $\lambda \to 0$ the resulting vortex shape is composed of parabolic sections depending on the previous magnetic history. The lower section of the vortex remains rigidly pinned, thus $x = y = 0$ for $z \leqslant z_0$. For example, when the tip moves along x and the dragging force F_x increases (but $F_y = 0$), one has $x(z) = (f_{px}/2\varepsilon_{lx})(z - z_0)^2$ for $z > z_0 = |F_x|/f_{px}$ where ε_{lx} is the vortex line tension for tilt along x and f_{px} is

* Corresponding author.
E-mail address: ehb@mf.mpg.de (E.H. Brandt).

0921-4534/$ - see front matter © 2010 Elsevier B.V. All rights reserved.
doi:10.1016/j.physc.2010.02.030

the pinning force density along x (see below). We note that at the surface $x_0 = x(0) = F_x^2/(2\varepsilon_{lx} f_{px})$, and thus the vortex-end shift deviates from Hook's law. At the surface one also has $x'(0) = F_x/\varepsilon_{lx}$ for small λ. When at some $x_0 = x_m$ the applied force F_x reaches its maximum F_m and begins to decrease, then the vortex shape is composed of two parabolic sections, and x_0 moves backward and tends to the value $x_m/2$ when $F_x \to 0$.

Finite λ causes the vortex to end perpendicular at the surface $z = 0$, thus $x'(0) = y'(0) = 0$. For simple history and small tilt angles the resulting shapes $x(z)$ and $y(z)$ may be calculated analytically. At larger tilt angles and when pinning and line tension are anisotropic (depending on the vortex orientation described by two angles), the detailed theory [2,6] shows that the critical force at which the vortex starts to move depends on the angle of the vortex tilt and in general does not coincide with the pinning force even in uniaxial superconductors. Thus, in the force balance for the vortex elements it is necessary to use this critical force instead of the pinning force. Our computations show that this effect together with the in-plane anisotropy $\zeta > 1$ further enhances the observed anisotropy of the vortex response during wiggling.

Fig. 1 shows this vortex wiggling. At time $t = 0$ the tip starts from $X = Y = 0$ oscillating along x with amplitude $a = 1.6$ (length unit micrometer) and at each quarter period the tip moves along y a small distance $c_y = 0.03$. The vortex end follows with some delay on a zigzag path to a maximum y, then it recedes to lower y and comes to a halt when the tip is too far away. In Figs. 1–5 the input parameters are: $\lambda = 0.2\ \mu\text{m}$, $\varepsilon_{lxy} \equiv (\varepsilon_{lx}\varepsilon_{ly})^{1/2} = 9$ pN, $P = f_p^c \lambda/\varepsilon_{lxy} = 0.5, q/\varepsilon_{lxy} = 1.1\ \mu\text{m}^2$, and $Z + h_0 = 0.44\ \mu\text{m}$. The pinning force densities along x or y are $f_{px} = f_p^c\sqrt{\zeta}$ and $f_{py} = f_p^c/\sqrt{\zeta}$, where f_p^c is the pinning force density for a vortex directed along the c axis in a uniaxial superconductor. The in-plane anisotropy is $\zeta = 1.3$ in Fig. 1b, while Fig. 1a shows the case with no in-plane anisotropy, $\zeta = 1$. Both x_0 and y_0 slightly recede after they have reached extremal values. The maximum excursions for $\zeta = 1(1.3)$ are: $x_m = \max(|x_0|) = 0.483(0.313)$, $y_m = \max(y_0) = 1.03(1.19)$. The aspect ratios of the approximate ellipse covered by the path of the vortex end is thus $r = y_m/x_m = 2.14(3.80)$. Thus, even in the absence of in-plane anisotropy this aspect ratio is $r = 2.14 > 1$. For large anisotropy $\zeta = 1.5$ we find $r = 5.5$. This ratio r of the maximum excursions of the vortex end is large since the x wiggling leads to some kind of a "drift" of the vortex end along y. This drift is similar to the drift in the "longitudinal vortex shaking" effect of Ref. [7].

Fig. 2 shows some vortex profiles $x(z)$ and $y(z)$ at selected times in Fig. 1b ($\zeta = 1.3$). One can see that the x wiggling leads to a large straight section in the widest profile $y(z)$ ($0 \leqslant y \leqslant 1.19$), which means that the y component of the pinning force is practically equal to zero along this section. The profiles $x(z)$ do not exhibit such a straight section, and their depinned section $|x(z)| > 0$ penetrates less deep than the section $|y(z)| > 0$. Actually, a closer look reveals that $x(z)$ performs a few spatial oscillations down to $z = z_0$,

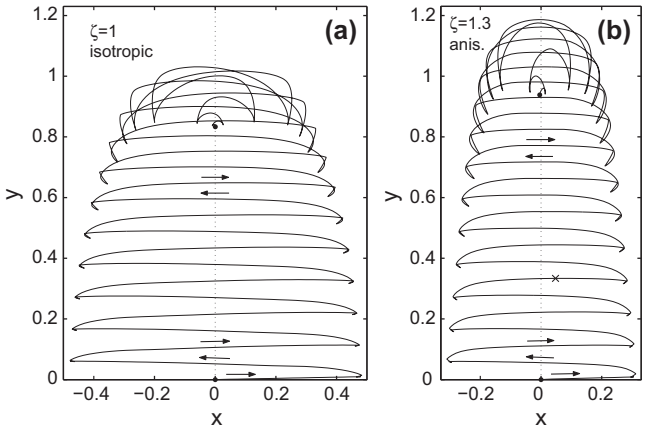

Fig. 1. The zigzag path $x_0(t)$, $y_0(t)$ of the vortex end at the surface $z = 0$ when the magnetic tip is oscillated at a height Z above the surface between $X = -a$ and $X = +a$ and slowly moves from $Y = 0$ to higher Y. Here $Z + h_0 = 0.44$, $\lambda = 0.2$, and $a = 1.6$, all lengths in micrometer. (a) No in-plane anisotropy ($\zeta = 1$). (b) $\zeta = 1.3$.

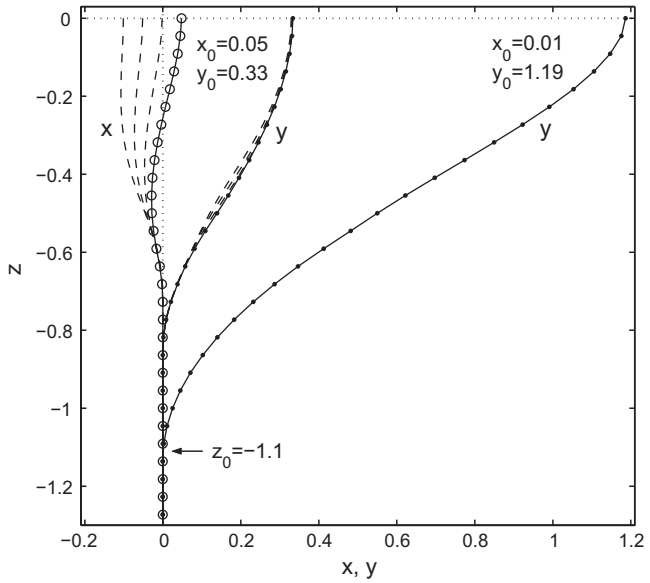

Fig. 2. The vortex shape during the wiggling of Fig. 1b expressed as $x(z)$ (solid line with circles) and $y(z)$ (solid line with dots) at the two moments when $x_0 = 0.05$, $y_0 = 0.33$, marked by a cross in Fig. 1b, and when the maximum $y_0 = 1.19$ is reached near $x_0 = 0$. The dashed lines show $x(z)$ and $y(z)$ at three previous times. At $z \leqslant z_0 = -1.1$ one has $x = y = 0$. All lengths in micrometer.

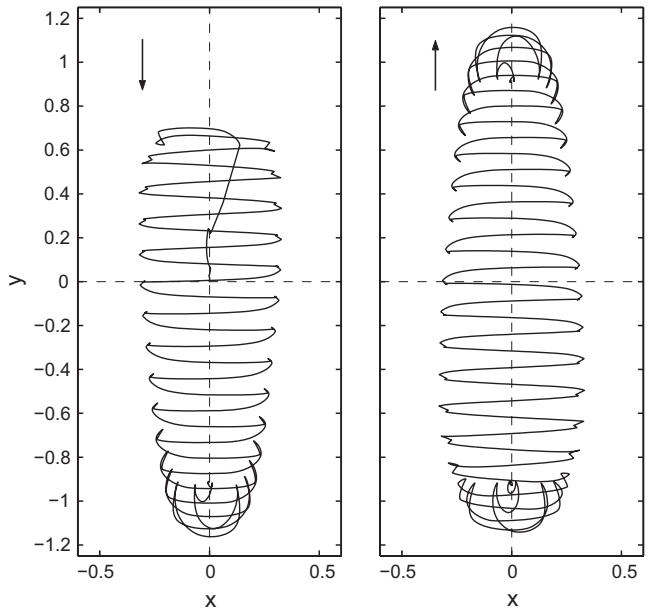

Fig. 3. The path of the vortex end when the tip oscillates along x with large amplitude and moves down from large positive $Y \geqslant 2$ (in micrometer) to large negative $Y \leqslant -2$ (left plot) and then moves up again to large positive $Y \geqslant 2$ (right plot). A pinned straight vortex waits at $x = y = 0$. When the tip approaches from above, the vortex end suddenly jumps towards the tip and starts to oscillate with large amplitude, following the tip downwards until it comes to a halt as in Fig. 1. When the oscillating tip approaches again from below, the vortex end starts to oscillate again along a path that looks similar to the path on which the vortex end came to a halt before.

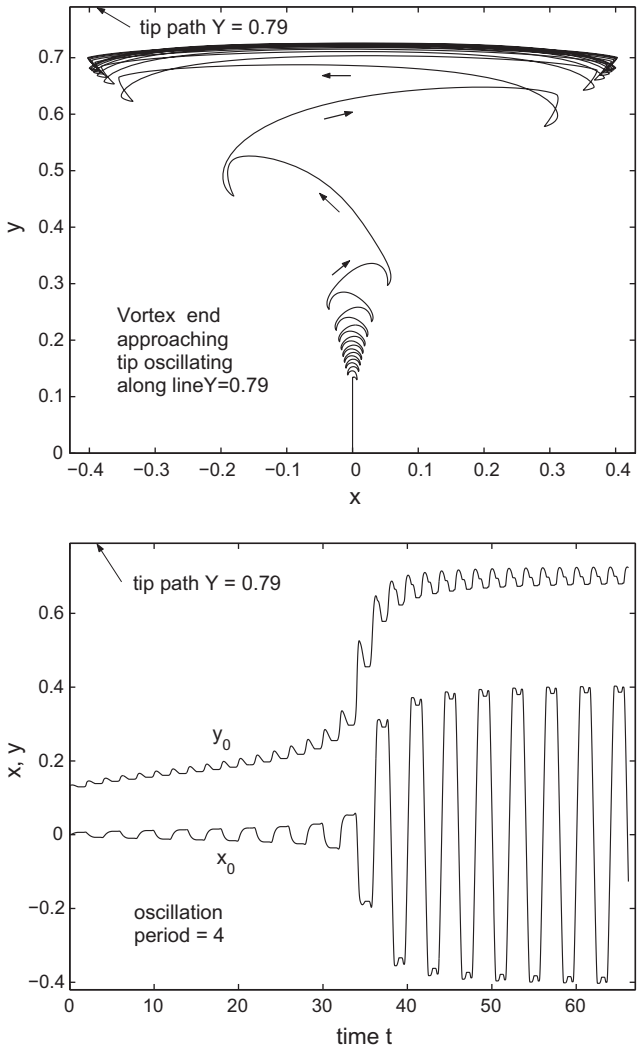

Fig. 4. Attraction of the vortex end to the tip oscillating with large amplitude $a = 1.4$ along the straight line $Y = 0.79$ parallel to the x axis, starting from $X = 0$ at time $t = 0$. When the tip approaches the starting point from large positive Y, the vortex end jumps from $y_0 = 0$ to $y_0 \approx 0.11$, attracted by the tip. At $t > 0$ the vortex end oscillates along x with small, slightly increasing amplitude, moving slowly to higher y values. When $y_0 \approx 0.3$ is reached the vortex end jumps in a few big leaps to its maximum $y_0 \approx 0.73$. After that it oscillates on a stationary curve. The lower plot shows the temporal dependences of x_0 and y_0. All lengths in micrometer, the unit of t is a quarter of the tip period, the parameters are as in Figs. 1–3, but for simplicity we take $\zeta = 1$ here. See also Fig. 12 of [2], where $Y = 0.8$, else same parameters.

but they are strongly damped and become visible only with magnification of 100 or 1000 times. At depths $z \leqslant z_0 = -1.1$ the vortex remains rigidly pinned at its original position $x = y = 0$ for all times.

In Fig. 3 a different scenario is shown but for same parameters as in Fig. 1b and 2. The oscillating tip now approaches the vortex from large positive Y, goes to large negative Y, and returns to large positive Y. This scenario is close to the experiments in [1] where the vortex positions are not known beforehand. The resulting path of the vortex end in Fig. 3 looks similar as in these experiments.

Fig. 4 shows the scenario when the magnetic tip oscillates along a straight line, $Y = 0.79$ with large amplitude. For $Y = 0.79$ the vortex end performs about nine small oscillations along x and moves slowly to higher y, then it jumps in about three big leaps towards the tip and reaches a stationary oscillating path with maximum $y_0 \approx 0.72 < Y$.

When the tip distance Y is only slightly increased to $Y = 0.80$, the number of oscillations (≈32) before the vortex end jumps towards

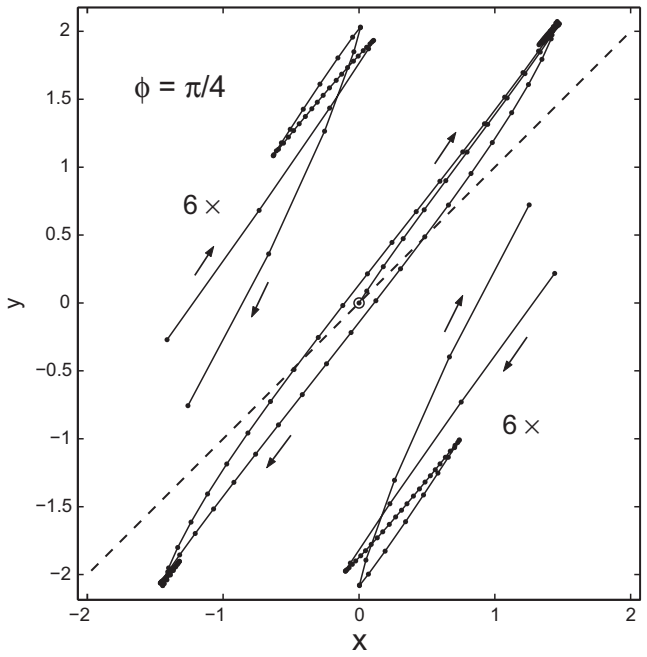

Fig. 5. Hysteretic path of the vortex end $x_0(t)$, $y_0(t)$ when the tip oscillates along the diagonal $X(t) = Y(t)$ (dashed line) with a large amplitude. Both the tip and the vortex start at $x = y = 0$. Length unit is λ, $P = 0.5$. The vortex end performs a narrow hysteresis loop that is tilted away from the tip-path towards the y axis since $\zeta = 1.3 > 1$. Also depicted is the six times enlarged and shifted path near the first and the second turns. The dots on the curves are at equidistant times.

the tip is drastically increased. For $Y = 0.805(0.81)$ the jump occurs after 75(375) oscillations, and at higher Y the maximum y_0 saturates exponentially in t to a small value $y_{0,\max} \approx 0.114$ and does not jump, see Fig. 13 in [2].

Fig. 5 shows the trajectory of the vortex end when the tip oscillates along the diagonal $X = Y$. It is seen that the vortex end performs a narrow hysteresis loop which is oriented at an angle >45° due to the in-plane anisotropy $\zeta = 1.3 > 1$.

The results of our calculations reproduce many features of the experimental data [1]. In particular, we compute the maximum displacement r_m of the vortex when the tip moves along a straight

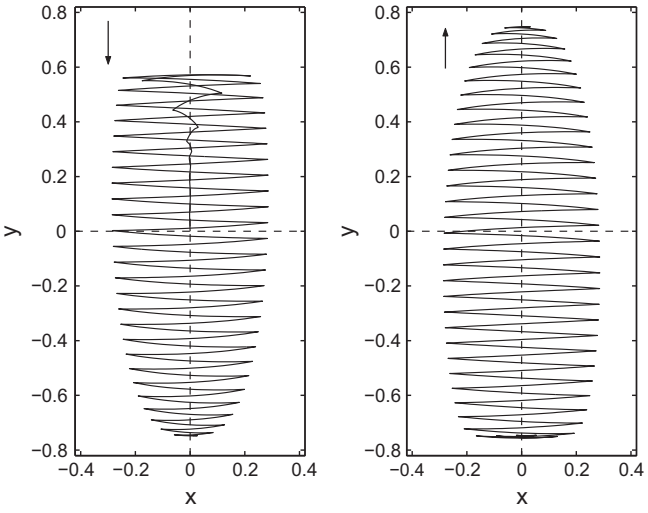

Fig. 6. Path of the vortex end for a simple two-dimensional model (see text) when the oscillating tip approaches from large $Y \geqslant 1.4$, goes to $Y \leqslant -1.4$ (left plot) and then returns to large $Y \geqslant 1.4$ (right plot), scenario of Fig. 3. Unit length is the effective tip height $Z + h_0 = 1$.

line tilted at the angle ϕ to the x axis and the position R_m at which $\partial F_z/\partial z$ reaches its maximum on the returning path of tip along the same line (at this R_m the tip is just above the vortex end). Such calculations give the dependence $R_m(\phi)$ for a fixed maximum driving force $F_m = 0.385q/(Z + h_0)^2$. We also calculated the dependence of R_m on F_m for the tip moving along the x axis or the y axis, and the hysteresis behavior of $\partial F_z/\partial z$ versus the tip position Y (at $X = 0$). All these theoretical results are similar to the appropriate experimental data presented in [1].

Finally, we show that the origin of the anisotropic vortex motion can be qualitatively understood from a simple two-dimensional (2D) model considering only the position of the vortex end (x_0, y_0). Assume that on this point act the dragging force $\mathbf{F}$, Eq. (1), the pinning force $\mathbf{F}_p$, and an elastic force $\mathbf{F}_{el} = (kx_0, ky_0)$ that pulls the vortex end towards the origin (0,0). The force balance $\mathbf{F} + \mathbf{F}_{el} + \mathbf{F}_p = 0$ then yields wiggling figures that look similar to the correct 3D results in Figs. 1 and 3. Fig. 6 shows the scenario of Fig. 3 for this two-dimensional model. Here we choose the effective tip height $Z + h_0$ as unit length and put $q = 1$, which determines the force unit. The other parameters in Fig. 6 are the spring constant $k = 0.3$ and pinning force $|\mathbf{F}_p| = 0.3$. This choice of parameters in this isotropic two-dimensional model yields for the scenario of Fig. 1 the maximum shifts $x_m = 0.283$, $y_m = 0.804$, and their ratio $r = y_m/x_m = 2.8$.

Acknowledgements

This work was supported by the German Israeli Research Grant Agreement (GIF) No. G-901-232.7/2005. EZ acknowledges the support of EU-FP7-ERC-AdG and of US-Israel Binational Science Foundation (BSF).

References

[1] O.M. Auslaender et al., Nat. Phys. 5 (2009) 35.
[2] E.H. Brandt, G.P. Mikitik, E. Zeldov, Phys. Rev. B 80 (2009) 054513.
[3] G. Carneiro, E.H. Brandt, Phys. Rev. B 61 (2000) 6370.
[4] U.H. Pi et al., Appl. Phys. Lett. 85 (2004) 5307.
[5] E.H. Brandt, Rep. Prog. Phys. 58 (1995) 1465–1594.
[6] G.P. Mikitik, E.H. Brandt, Phys. Rev. B 79 (2009) 020506(R).
[7] G.P. Mikitik, E.H. Brandt, Phys. Rev. B 67 (2003) 104511.